2024

Economic heavy minerals in the stream sediments of wadi Shaàb, southern coast of the Red Sea, Egypt; characterization and upgrading for investigation of their potential recovery

Mona FAWZY
mm1_fawzy@yahoo.com

Mustafa BAYOUMI
moustafanma@yahoo.com

Hassan SHAHIN
hassanshahin03@yahoo.com

Bahaa EMAD
prof_bahaa24@yahoo.com

Abdel Hay EL SHAFEY
abdelshafey48@gmail.com

Economic heavy minerals in the stream sediments of wadi Shaàb, southern coast of the Red Sea, Egypt; characterization and upgrading for investigation of their potential recovery

Authors

Mona FAWZY, Mustafa BAYOUMI, Hassan SHAHIN, Bahaa EMAD, Abdel Hay EL SHAFEY, Marwa ABDEL-AZEEM, Ahmed ISMAIL, Asmaa EL-MOGHAZY, and Mohamed DIAB

Bulletin of the Mineral Research and Exploration

http://bulletin.mta.gov.tr

Economic heavy minerals in the stream sediments of wadi Shaàb, southern coast of the Red Sea, Egypt; characterization and upgrading for investigation of their potential recovery

Mona FAWZY[a*] , Mostafa BAYOUMI[a] , Hassan SHAHIN[a] , Bahaa EMAD[a] , Abdel Hay EL SHAFEY[a] , Marwa ABDEL-AZEEM[a] , Ahmed ISMAIL[a] , Asmaa EL-MOGHAZY[b] and Mohamed DIAB[a]

[a] *Nuclear Materials Authority, P. O. Box 530, Maadi, Cairo, Egypt*
[b] *Geology Department, Faculty of Science, Helwan University, Ain Helwan, 11795, Cairo, Egypt*

Research Article

ABSTRACT

The southern coast of the Red Sea is one of the most promising areas for the occurrence of economic minerals. Therefore, studying the characterization and evaluation of these minerals in the Wadi Shaàb Quaternary sediments and investigating their ability to concentrate and physically separate using economical and ecofriendly techniques is the main goal of this work. The results showed that the representative sample contains an average of 0.06% ilmenite, 0.08% zircon, 0.07% rutile, 0.07% leucoxene, 0.008% cassiterite, 0.004% xenotime, 0.0004% monazite, 0.022% almandine garnet, and 0.46% magnetite. The recovery of economic heavy minerals was applied using a combination of wet-gravity technique via shaking table and magnetic separation using high intensity magnetic separator. The results demonstrated the success of gravity separation in raising the grade from 7.63% to 45.03% in a yield of 13.74% out of the original sample, and also valuable metallurgical recoveries that higher than 89% for tabling multi-stages (rougher and scavenging) was obtained. Concentrated mineral fractions of magnetite, ilmenite, almandine, heavy silicates, and the non-magnetic fraction bearing zircon and rutile were obtained using a high intensity magnetic separator at different ampere range.

1. Introduction

Zircon, ilmenite, rutile, and garnet are economic heavy minerals used as raw materials for nuclear energy production and also in the manufacture of metallurgical and engineering industrial products (Grosz and Schruben, 1994; Fawzy et al., 2022*a*), in addition to that, monazite and xenotime contain critical metals such as rare earth elements (REE) that have high-tech applications.

Normally, processing of heavy mineral sands does not require crushing and grinding operations, which reduces cost and saves energy (Jordens et al., 2013). Most mineral beneficiation techniques for sand raw material begin with gravity separation by exploiting the density differences between heavy and their associated light minerals, which consist mainly of quartz and feldspar (Moscoso-Pinto and Kim, 2021; Fawzy, et al., 2022*b*; Diab, et al., 2022). After gravity separation, highly magnetic minerals (ferromagnetic as magnetite) can be separated from the obtained heavy minerals using low intensity magnetic separator (LIMS) and also paramagnetic minerals can be separated from diamagnetic minerals via high intensity

magnetic separator (HIMS), electrostatic or flotation separation techniques can be also implemented depending on the properties of each mineral to be separated (Rejith, and Sundararajan, 2018; Fawzy, 2018; 2021*a*; *b*). Regarding magnetic separation, the mining industry is currently using this process for ore processing, material screening and mineral purification (Iranmanesh, and Hulliger, 2017). Therefore, it is essential to decide on the mineral processing that can recover the valuable heavy minerals (VHMs) with a fast and efficient processing rate. This research focuses on the efficient recovery of the economic heavy minerals in the stream sediments of the Wadi Shaàb area. Among their valuable minerals, we can find hematite, magnetite, ilmenite, leucoxene, xenotime, monazite, rutile, cassiterite, and zircon. To achieve the heavy mineral recovery, this study considered two sequential mineral beneficiation processes: Magnetic separation after gravity concentration techniques via variable magnetic field strengths to optimize the recovery and final grade of each VHMs.

2. Geological Setting and Sampling

The Wadi Shaàb area is located at the southeastern corner of Egypt about 30 km south Shalateen city between latitudes of 22° 33′ and 22° 55′ N, and longitudes of 35° 21′ and 36° 00′ E (Figure 1). The geomorphological units that were recorded in the study area are: high mountains, isolated hills, piedmont plain, alluvial fans, coastal plain and hydrographic basins (Yousef, et al., 2009). The high mountains of Wadi Shaàb area are composed mostly of ophiolitic rocks, metasediments, metavolcanics and related volcanoclastic, tonalite-granodiorite as well as biotite-muscovite granite. The piedmont plain and alluvial fans consist mainly of coarse sand, gravel, and pebbles which changed eastward to become fine to medium sand and silt. The coastal plain is represented mainly by sand sheets, sand dunes and sabkha deposits that parallel to the shoreline.

Systematic sampling patterns were carried out for the studied stream sediments of the Wadi Shaàb. Nineteen samples were obtained through pits arranged in two profiles in the middle of Wadi Shaàb (Figure 1). The pits are of about 50 cm diameter and 70 -100 cm depth and 1- 6 km apart (Figure 2).

3. Methodology

Each studied sample for the Wadi Shaàb stream sediments was prepared firstly by proper mixing and splitting into representative sub-samples to undergo various characterization tests, such as determination of grain size distribution, total heavy mineral (THM) concentration, measurement of apparent density. One test sample representing the area under investigation was equipped with a mass of about 15 kg by mixing an equal amount of each sample thoroughly. Various characterization tests were carried out for this sample in order to complete the physical concentration and separation of economic heavy minerals from the stream sediments. The methodology flowchart is shown in Figure 3. The grain size distribution analyses of the studied samples were performed by using mechanical sieve shaker with set of sieves with mesh diameters of 2.0, 1.0, 0.5, 0.250, 0.125, and 0.063 mm (ASTM codes). Each size fraction was weighed, and its distribution recorded. While the apparent density measurements were carried out by weighing the sample then pouring it inside a graduated cylinder, after that compacted well to simulate the presence of the sample in nature. The density values obtained from dividing the mass of the sample by its volume.

Heavy liquid separation tests were carried out using bromoform (CHBr$_3$; density 2.89 g/cm^3) with the aim of separating heavy minerals from the associated light minerals, which mainly consist of quartz and feldspar (densities 2.65 and 2.56 g/cm^3 respectively). This test was performed by placing 50 g of each sample in a separating funnel with the bromoform, stirring for 5 minutes and allowing it to stand for 15 minutes. Next, the heavy and light mineral fractions were separated, rinsed with acetone, dried and weighed. Each obtained heavy fraction was subjected to grain size distribution analyses and magnetic fractionation tests using mechanical sieve shaker and Carpco High Intensity magnetic separator (HIMS) respectively. Additionally, an Olympus stereo binocular microscope was also used to prepare and select pure mineral grains by hand picking. The mineralogical characterization for the obtained picked heavy mineral grains was carried out in this work via X-ray diffraction (XRD) instrument and environmental scanning electron microscope
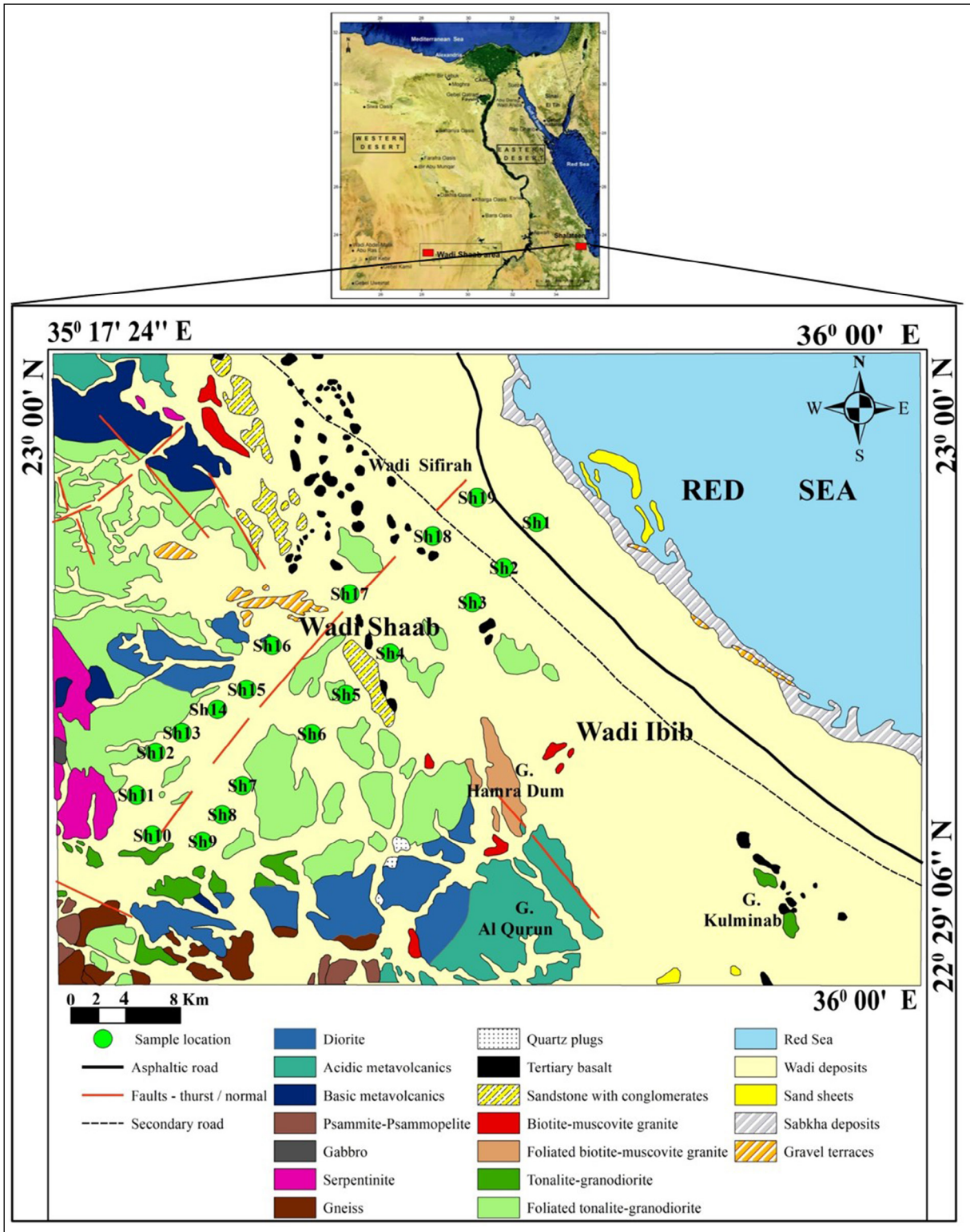
Figure 1- a) Location map of Shaàb area, and b) Geological map showing sampling locations of the Wadi Shaàb area, south Eastern Desert of Egypt (Modified after EGSMA, 2002).

Figure 2- Field photo showing the sampling techniques at the Wadi Shaàb area.

(SEM) (a Philips Model XL 30) that supplied with energy dispersive spectrometer (EDS) unit.

Chemical assays of the Shaàb samples were determined using an energy-dispersive X-ray fluorescence (EDXRF) Rigaku spectrometer with polarized optics. EDXRF is one of the most convenient and fast analytical methods suitable for working in physical beneficiation field (Rydberg, 2014; Zhao et al., 2020). The schematic flowsheet of heavy mineral estimation using EDXRF spectrometry was depicted at Figure 3.

Physical beneficiation experiments for the Shaàb test sample were carried out firstly via wet-gravity technique using shaking table (Wilfley, No. 13) to minimize the associated gangue (quartz and feldspar) at the lowest possible level. The obtained heavy concentrates were subjected to low intensity magnetic separator to separate magnetite. Free-magnetite heavy concentrates were subjected to high-intensity magnetic separator (Carpco, Model MLH, 13 III-5" 15) for separating paramagnetic from diamagnetic minerals. Magnetic separation processes were carried out at different magnetic currents of intensity at 0.8, 1.5, and 2 .5 A, pre-optimized factors of a medium air gap of 1.5 cm, average air gap of 1.5 cm, magnetic roll speed of 30 rpm and finally at
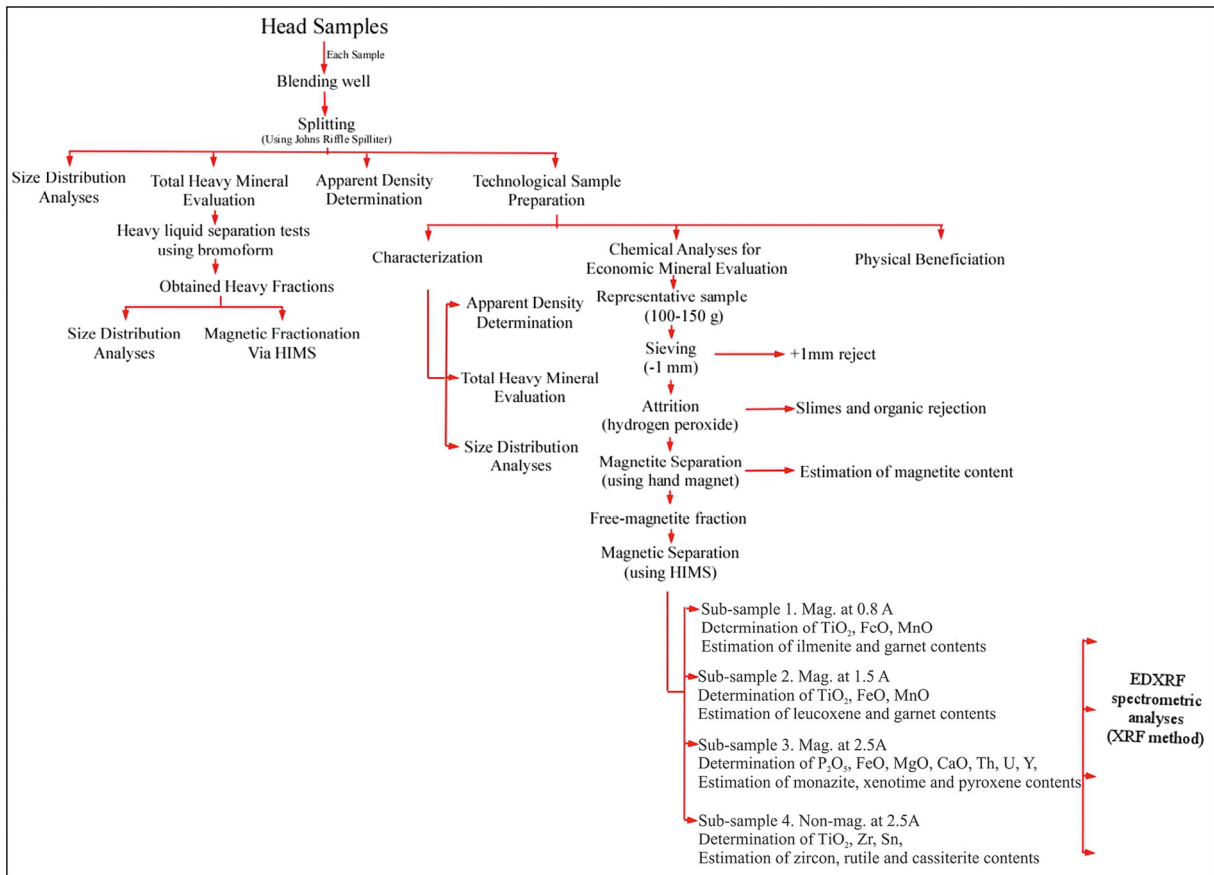

Figure 3- Methodology flow-sheet.

a feed rate of 39.2 g/min. About 100 grams of the obtained gravity concentration products (concentrate and tail) were subjected to bromoform separation test for heavy mineral assay estimation.

4. Results and Discussion

4.1. Sample Characterization

The EDXRF analyses for Shaàb head representitive sample were shown in Table 1, the head assays of the main oxides showed contents of Fe_2O_3 is 2.85% and TiO_2 is 0.41%. The highest trace elements are zirconium (355 ppm), Cr (435 ppm), and Ni (366 ppm) while Zn, Y, Pb, Cu, Nb, and Sn showing their low contents.

Size distribution analysis is the most important physical parameter that has a significant impact on the separation efficiency using various physical beneficiation techniques. Many research papers confirmed that the highest percentage of heavy minerals liberation was found in the size fraction less than 250 μm (Rahman et al., 2015; Hegde et al., 2006; Shalini et al., 2020; Paltekar et al., 2021). Grain size distribution analyzes results of the Wadi Shaàb head samples (Sh 1-19) as well as test sample (Sh tech.) were presented in Figure 4. It showed a high degree of homogeneity and the mean values confirmed that the highest percentage (73.4% mass) of the samples size is retained in a size ranging from 1 to 0.063 mm while the gravel and very coarse sand fractions were about 23.26% mass, and the silty size fraction was calculated as 3.33% mass. For Shaàb sample (Sh tech.), it was 73.03% mass for size range from 1to 0.063mm, 24.71% mass for the gravel and very coarse sand fraction, and 2.27% mass for the silty size fraction.

Table 1- EDXRF analyses of Shaàb head bulk sample.

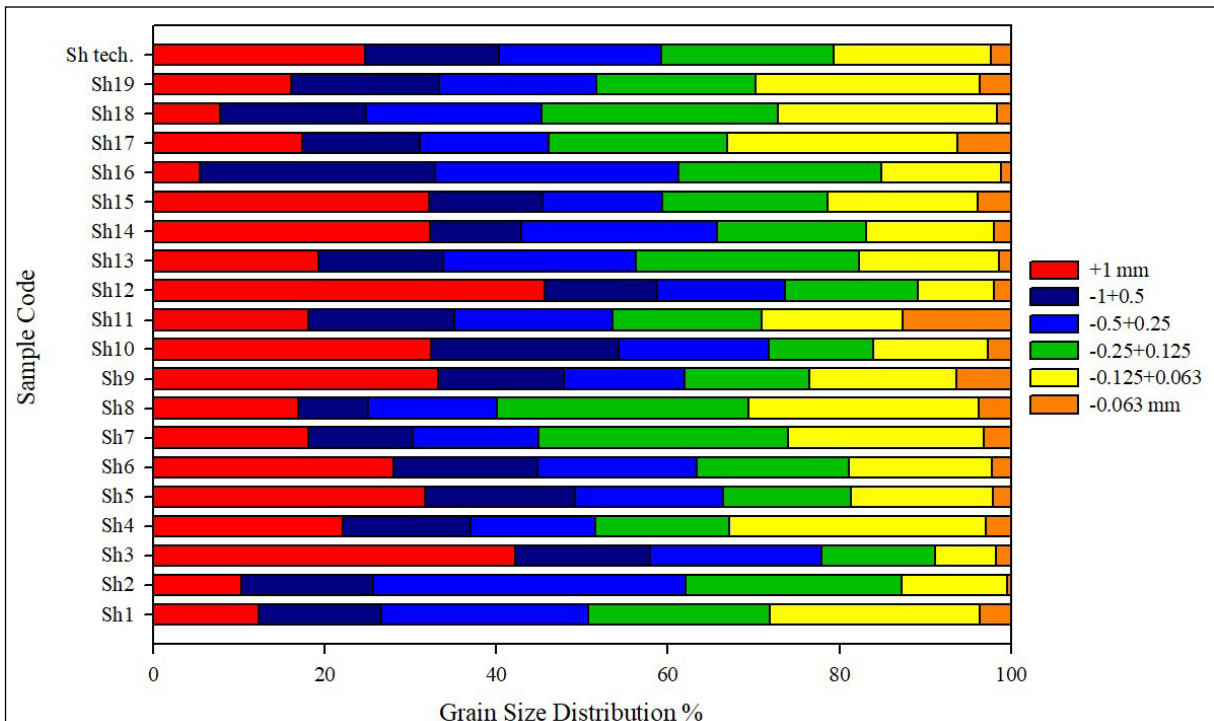| Major Oxides (%)						Trace Elements (ppm)										
Fe_2O_3	CaO	TiO_2	P_2O_5	K_2O	MnO	Zr	Cr	Ni	Co	V	Zn	Y	Pb	Cu	Nb	Sn
2.85	2.32	0.41	0.09	0.81	0.05	355	435	366	110	142	65	21	11	28	11	58.9

Figure 4- Grain size distribution analyses for the Shaàb stream sediment samples.

The apparent density values were used as evidence for the presence of heavy mineral concentrations in the studied samples; in addition to using these values for estimation the reserves of heavy minerals in the area under investigation (Fawzy et al., 2022*a, b*; Diab et al., 2022). As for the apparent density measurements of the Wadi Shaàb samples which were shown in Figure 5, the values ranged between 2.46 g/cm³ for sample no.10 (Sh10) to 1.21 g/cm³ for Sh14, with an average of about 1.86 g/cm³ and the value of the Shaàb sample was 1.83 g/cm³. Compared to the typical values of dry density of ordinary sand, which is estimated at 1.5 g/cm³ (Yu et al., 2023), this indicates that the raw Shaàb sand contains heavy minerals in a higher proportion than ordinary sand. The content of the heavy minerals in each sample was determined using a heavy liquid separation (bromoform) technique, and the results were showed in Figure 6. The results confirmed that the total heavy mineral content in the Shaàb samples ranged between 2.91% mass for Sh 9

and 11.24% mass for Sh 13, with an average of about 8.00% mass and 7.63% mass for Sh tech.

The obtained heavy mineral fractions were studied for size distribution analysis and the results were presented in Figure 7, the mean results (for 19 samples) showed that 96.08% mass of the HMs retained in the size range 1 to 0.063 mm while zero percent of HMs in the size fraction greater than 1mm and 3.91% mass of HMs presented in silt size fraction (-0.063 mm). The results for the Shaàb test sample were as follows, 96.86% mass of HMs kept in size fraction -1+0.063 mm, 0% mass in +1mm size fraction, and 3.13% mass of the HMs in silty fraction. Figure 7 also shows that the mineral fraction (-0.125 + 0.063mm) is the largest fraction that retains heavy minerals (about 40%), followed by fraction (-0.25 + 0.125 mm) that retained about 30% of the heavy minerals.

Microscopic examination for the picked heavy mineral grains using Stereo-binocular microscope
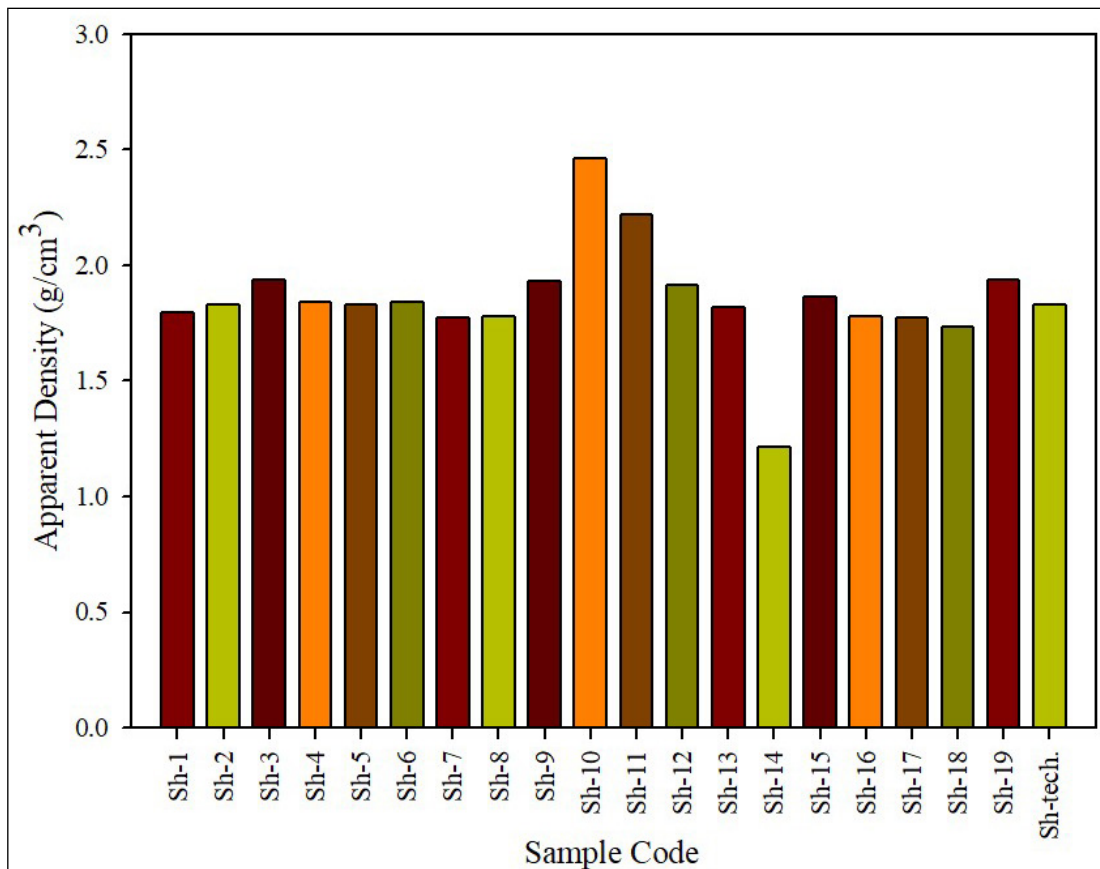

Figure 5- Apparent density measurements in the Wadi Shaàb stream sediment samples.
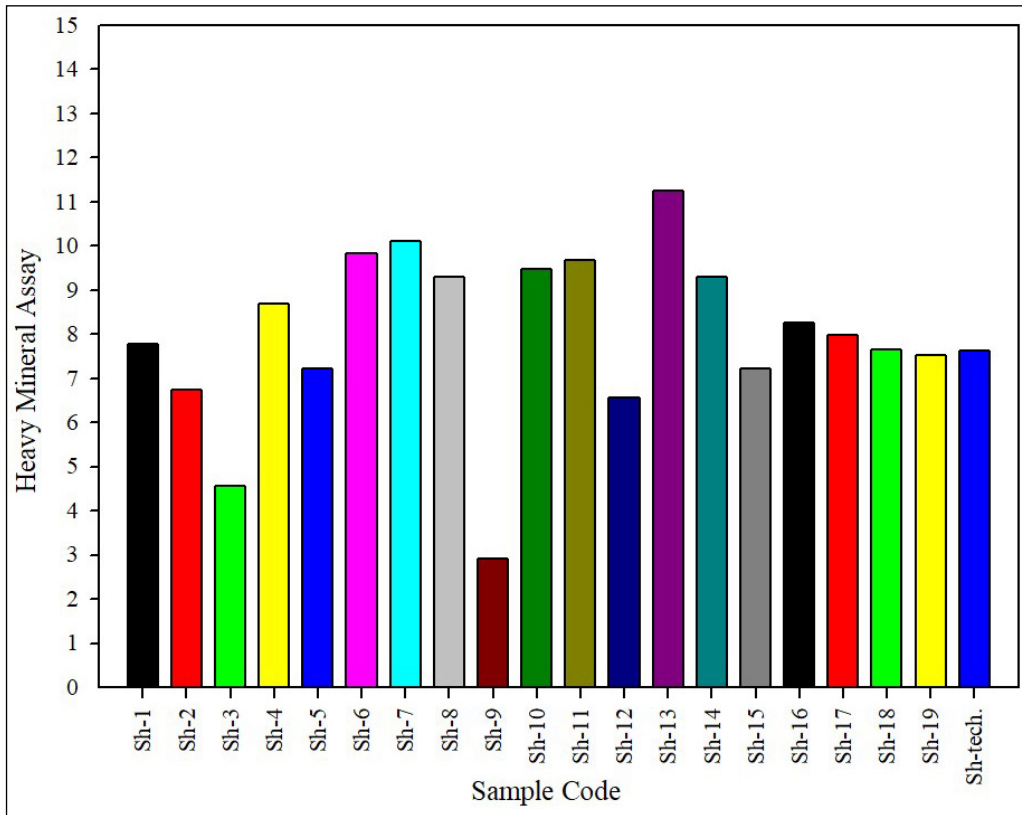
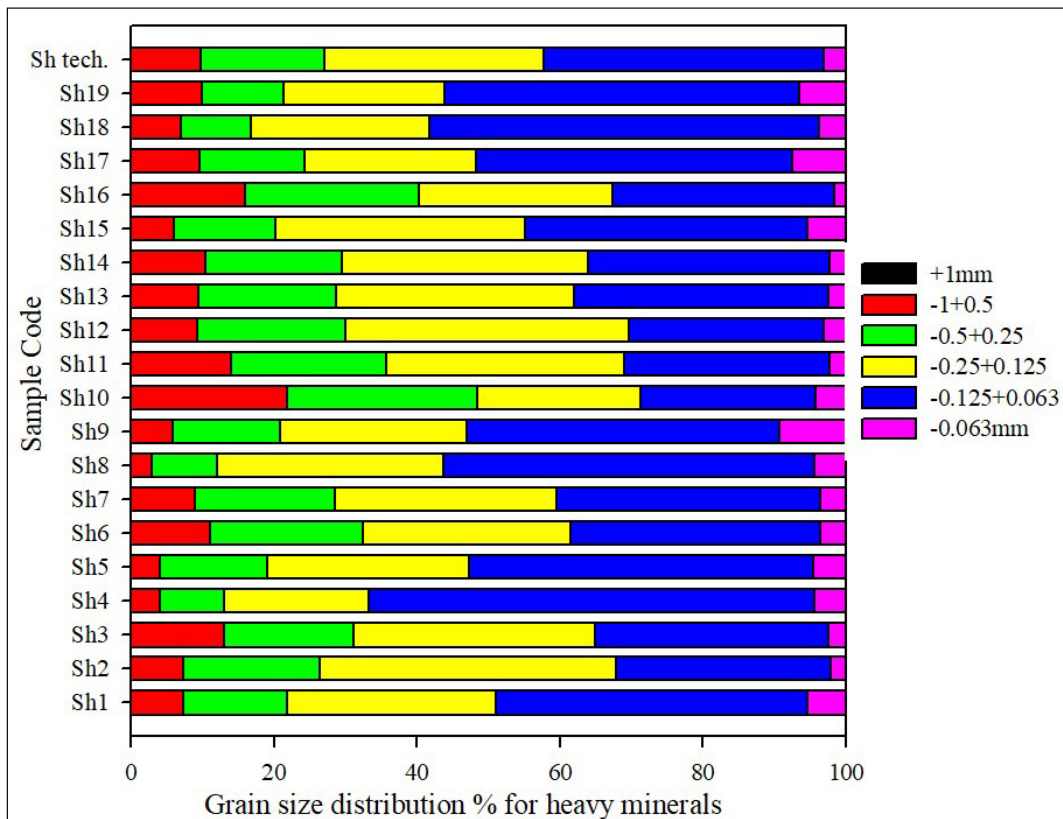Figure 6- Heavy mineral distribution analyses for the Shaàb samples.

Figure 7- Size distribution analyses for the Shaàb heavy mineral fractions.

then SEM analyses that supplied with EDS unit revealed the presence of a large group of economic heavy minerals that were listed as follows; ilmenite (Figure 8a), leucoxene (Figure 8b), rutile (Figure 8c), sphene (Figure 8d), zircon (Figure 9a), Zn-Sn-Pb mineral (Figure 9b), Zn mineral (Figure 9c), xenotime (Figure 10a), monazite (Figure 10b), cassiterite (Figure 10c).

For detailed mineralogical study, magnetic fractionation for the separated heavy minerals was conducted using HIMS magnetic separator. Each heavy mineral sample was magnetically separated into five fractions (magnetic at 0.04A, 0.8A, 1.5A, 2.5A, and non-magnetic at 2.5A). Each fraction was weighted and calculated with respect to the percentage of heavy minerals and the results are presented in Figure 11. The magnetic fractionation results manifested that the magnetic fraction at 1.5A represents the highest value ranging from 30.61% mass for Sh 14 to 58.93% mass for Sh 7 with an average of about 46.19% mass followed by the magnetic fraction at 2.5A, where the values ranged between 8.29 % mass for Sh 4 to 27.94% mass for Sh 14 with an average of 17.76% mass. While the non-magnetic fraction at 2.5A has values between 10.48% mass for Sh 6 to 24.85% mass for Sh 14 with an average of 17.12% mass. The magnetic fraction at 0.8A, its value ranged between 8.79 to 26.10% mass with an average of 14.15% mass. As for the lowest value of magnetic fractionation, it had a magnetic fraction of 0.04A which ranged from 2.09 to 7.81% mass with an average of 4.78% mass. With regard to the Shaàb test sample, the magnetic fractionation results were as follows; 54.61% mass for magnetic fraction at 1.5A, 26.61% mass for magnetic fraction at 2.5A, 4.03% mass for non-magnetic fraction at 2.5A, 8.44% mass for magnetic fraction at 0.8A, and 6.32% mass for magnetic fraction at 0.04A (Figure 11).

EDXRF analyses for the oxides and elements of different magnetic fractions for the Shaàb test sample were shown in Table 2. The data of analyses as well as magnetic fractionation results in order to compute the contents heavy minerals assuming their stoichiometric composition, revealed that the content of ilmenite reaches 0.06%, zircon is 0.08%, rutile is 0.07%,

leucoxene is 0.07%, cassiterite is 0.008%, xenotime is 0.004%, monazite is 0.0004%, heavy silicates is 0.53%, almandine is 0.022%, and magnetite represents 0.46%.

The mineralogical confirmation of the magnetic fractionation of the Wadi Shaàb representative sample was conducted via x-ray diffraction analyses and the diffractograms for the various fractions were depicted in Figure 12 and Figure 13. Figure 12a showed that the magnetic fraction at 0.04 amps contains mainly magnetite, hematite, and antigorite which have ASTM Card No. 76-1849, 58-599, and 44-1447 respectively. While the magnetic fraction at 0.8 amps was mainly composed of ilmenite, hematite and actinolite which have ASTM Card No. 03-778, 01-1053 and 85-2157 respectively (Figure 12b). The alteration product of ilmenite (leucoxene), actinolite, almandine, quartz and traces of rutile separated as magnetic fraction at 1.5 amps and have ASTM Card No. 03-778, 85-2157, 74-1553, 85-789, and 72-1148 respectively (Figure 12c).

Magnetic separation at 2.5 amps proved the presence of epidote, actinolite, and monazite, which have ASTM Card No. 17-514, 85-2157, and 46-1295 respectively (Figure 13a), while the non-magnetic fraction at the same amperes showed the presence of zircon, rutile, cassiterite, and diopside, which have ASTM Card No. 81-588, 72-1148, 77-449 and 83-98 respectively (Figure 13b).

4.2. Beneficiation Processes

Zircon, rutile, ilmenite and other economic minerals are found all over the world, but not always in high grade concentrations. Therefore, low-grade ores can be exploited by raising their grades via various physical beneficiation processes.

The beneficiation processes of the Shaàb test sample was firstly carried out by raising the grade of heavy minerals through the shaking table in order to get rid of quartz and feldspar as much as possible. The obtained heavy mineral concentrate was fed as feed to different magnetic separators to differentiate the minerals according to their magnetic response.
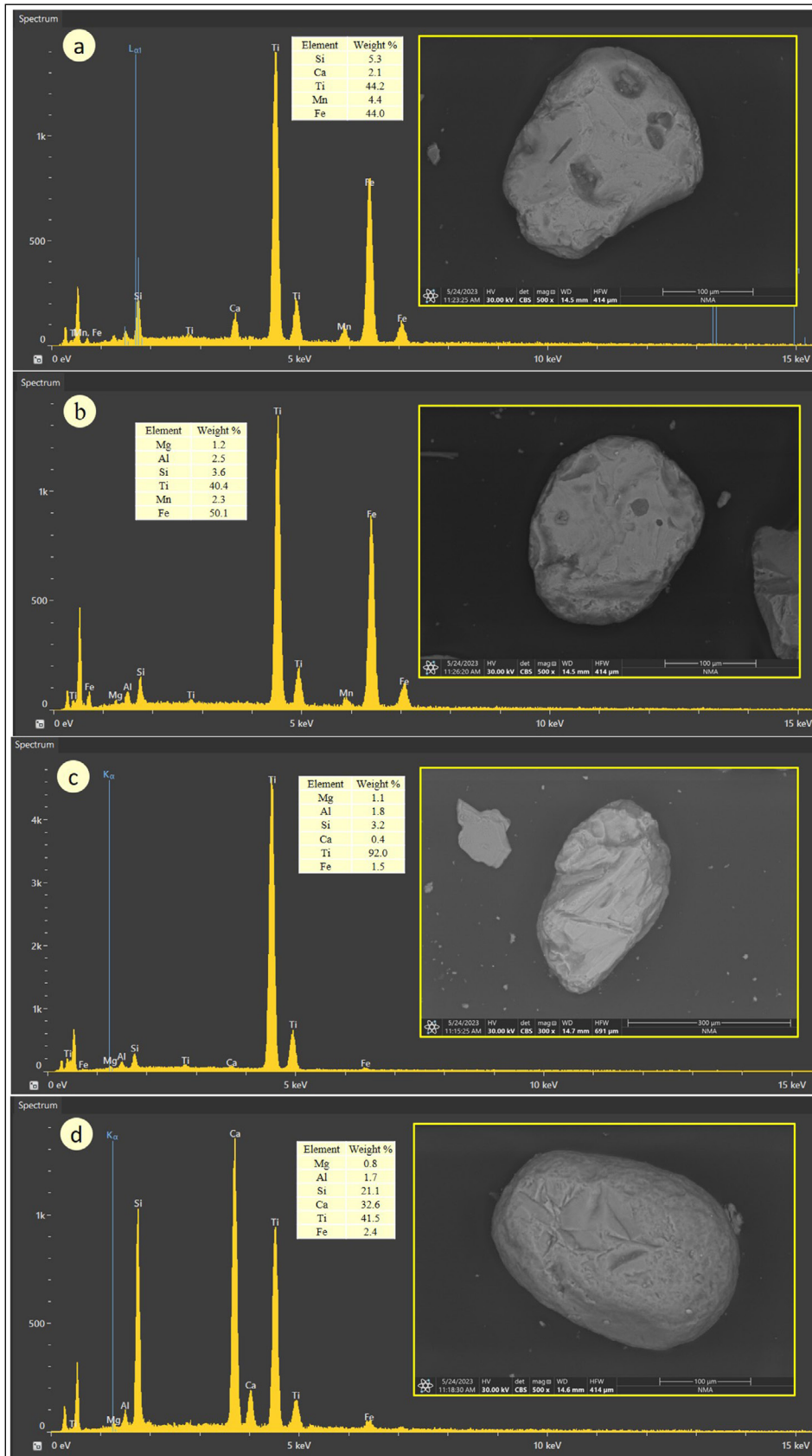
Figure 8- Back-scattered electron (BSE) images and corresponding EDS spectra showing; a) ilmenite, b) leucoxene, c) rutile, and d) sphene.
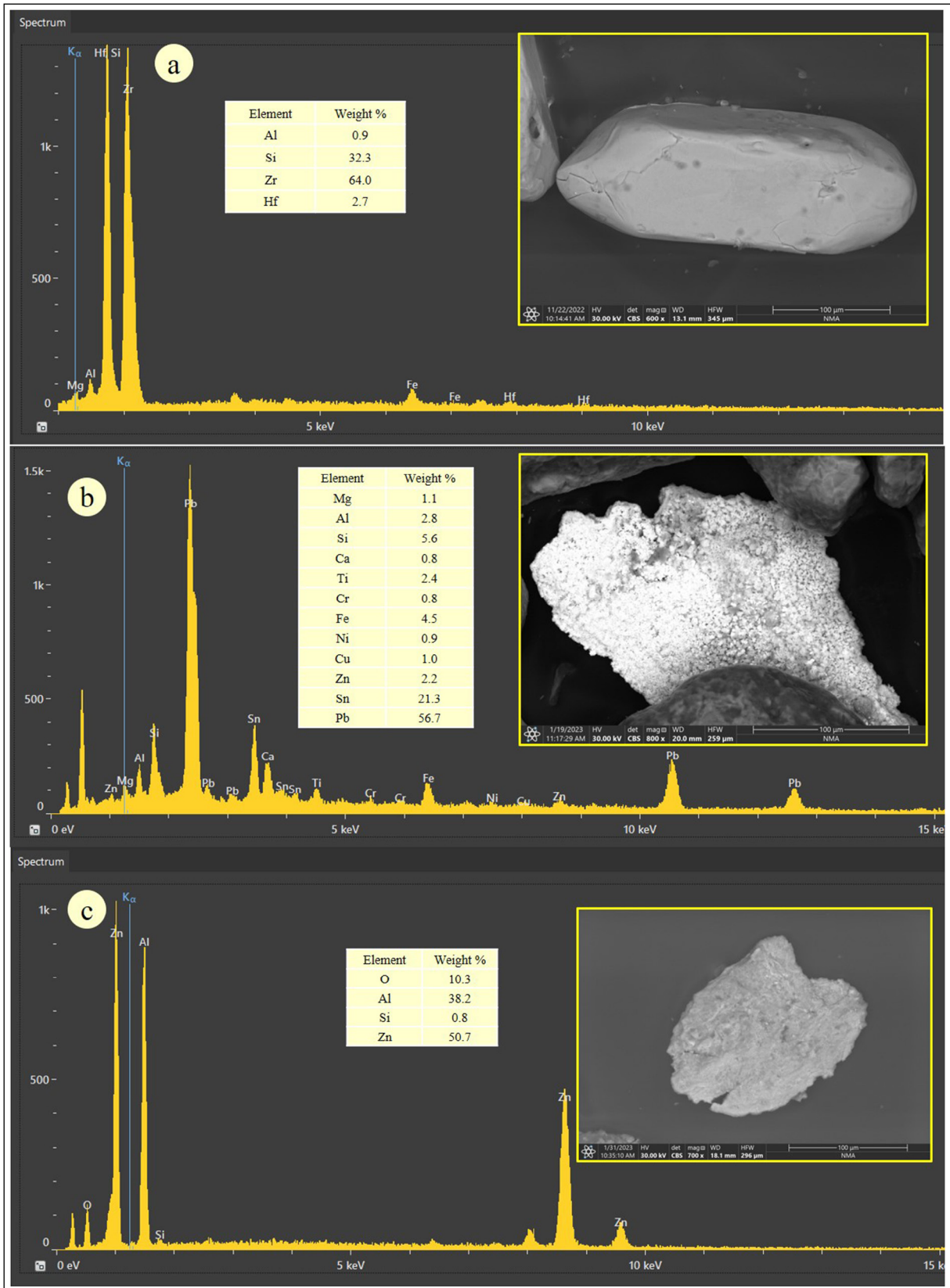
Figure 9- BSE images and corresponding EDS spectra showing; a) zircon, b) Zn-Sn-Pb mineral, and c) Zn-mineral.
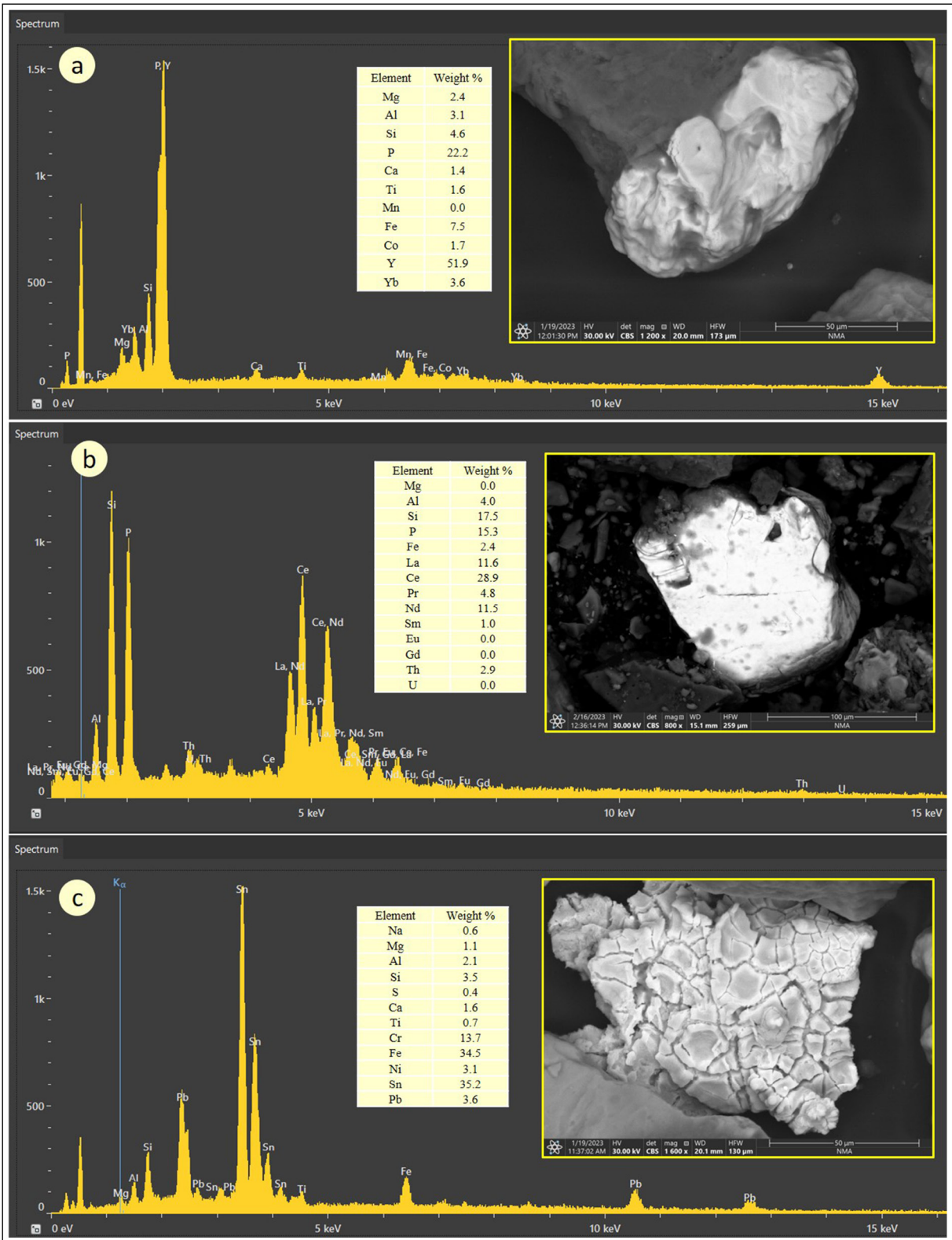
Figure 10- BSE images and corresponding EDS spectra showing; a) xenotime, b) monazite, and c) cassiterite.
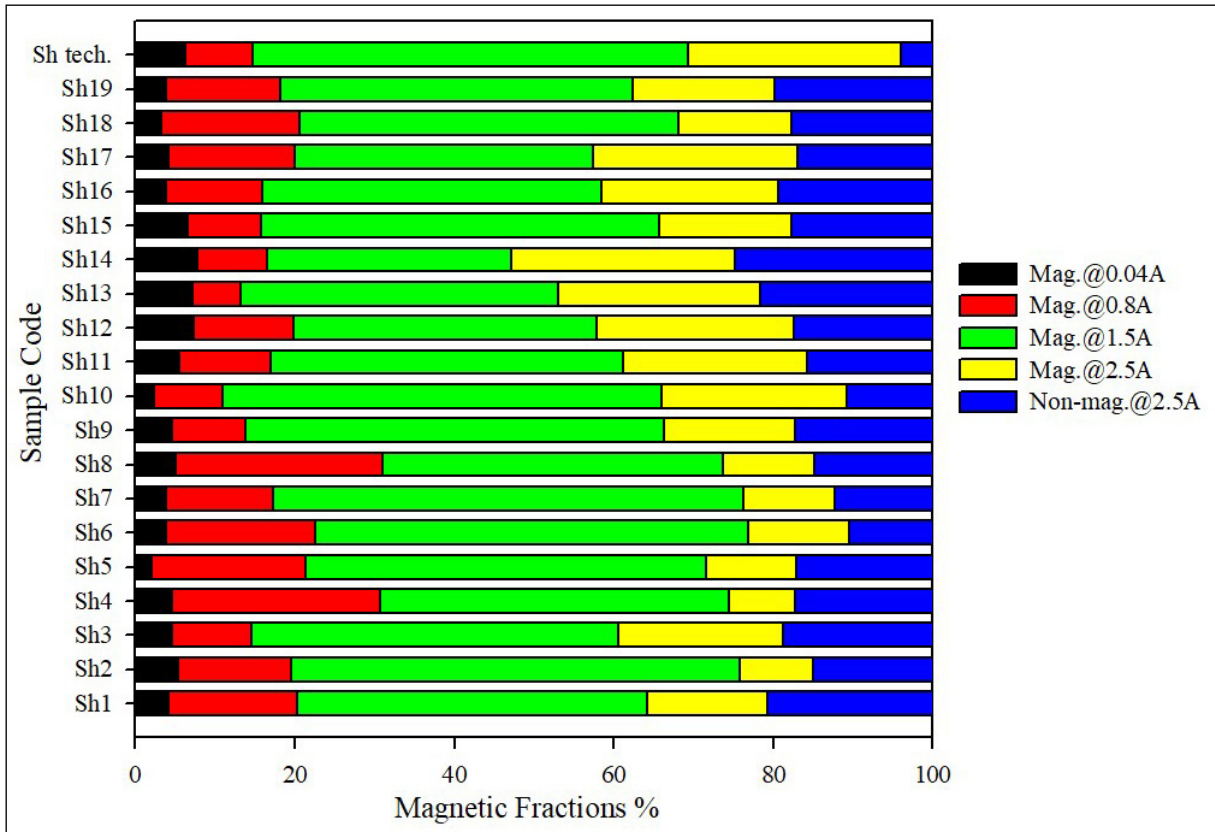
Figure 11- Magnetic fractionation for heavy mineral fractions in the Shaàb samples via DHIMS.

Table 2- EDXRF analyses of the Shaàb test sample after magnetic fractionation.

Shaàb Sample after Magnetic Separation	Mag. Fr. @0.8A	Mag. Fr. @1.5A	Mag. Fr. @2.5A	Non-mag. Fr. @2.5A
Major Elemental Oxides in %				
Fe_2O_3	9.3	10.8	8.12	0.932
CaO	1.14	3.32	3.81	2.27
TiO_2	1.44	1.13	0.887	0.167
P_2O_5	0.0755	0.08	0.084	0.087
K_2O	0.161	0.976	0.724	1.07
MnO	0.142	0.232	0.16	0.024
Trace Elements in ppm				
Cr	2740	490	563	46
Ni	1750	336	285	55
Co	510	327	280	37
V	324	339	266	45
Zn	114	191	143	42
Y	18	80	45	16.6
Pb	11	10	10.5	15.2
Cu	<0.1	80	<0.1	13.6
Th	<0.1	<0.1	9.5	<0.1
U	<0.1	<0.1	<0.1	<0.1

4.2.1. Shaking Table Concentration

Heavy minerals were concentrated from the sand by exploiting differences in mineral density via a rougher stage followed by multi-stages of scavengers through Wilfley Shaking Table No. 13 (Fawzy et al., 2022*a, b*). The rougher stage was carried out under optimum conditions of 134 g/min feed rate, 14 liters/min water flow rate, stroke length of 1.5 cm, and inclination angle of 9°, while the multi-

scavenging stages were carried out under operating conditions of 140 g/min feed rate, water flow rate of 17.5 liters/min., 2 cm stroke length, and inclination angle of 11°. It is clear from the aforementioned values that the scavenging stages have greater values for operating conditions than those for the roughing stage, due to the higher content of light minerals and lower content of heavy minerals during the scavenging stages. About 50 g representative sample of the
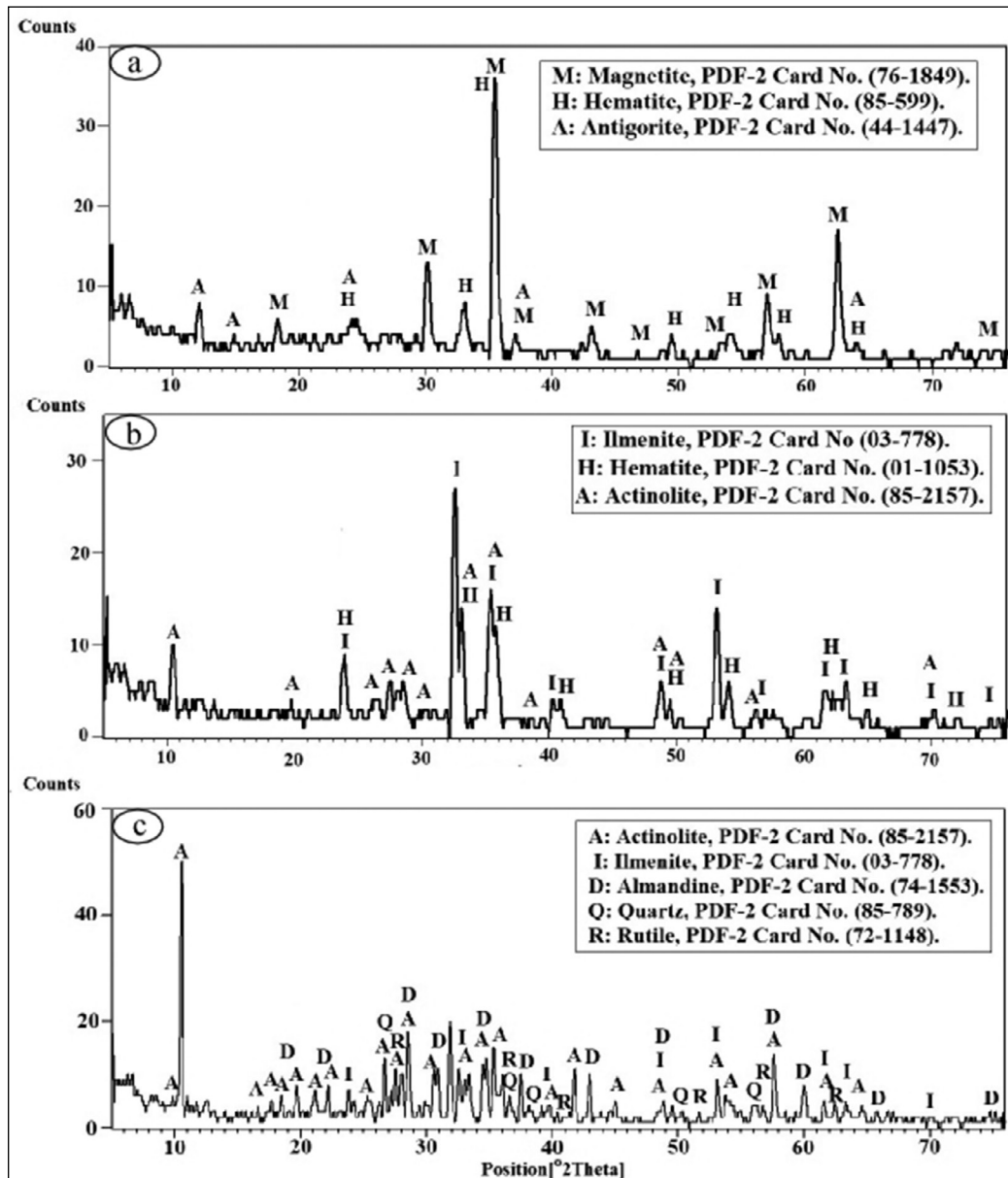

Figure 12- XRD diffractograms showing: a) magnetite, hematite, and antigorite separated as magnetic fraction at 0.04 amps, b) ilmenite, hematite, and actinolite separated at 0.8 amps as magnetic fraction, and c) almandine, ilmenite, actinolite, quartz, and rutile separated at 1.5 amps as magnetic fraction of the Wadi Shaàb representative sample.
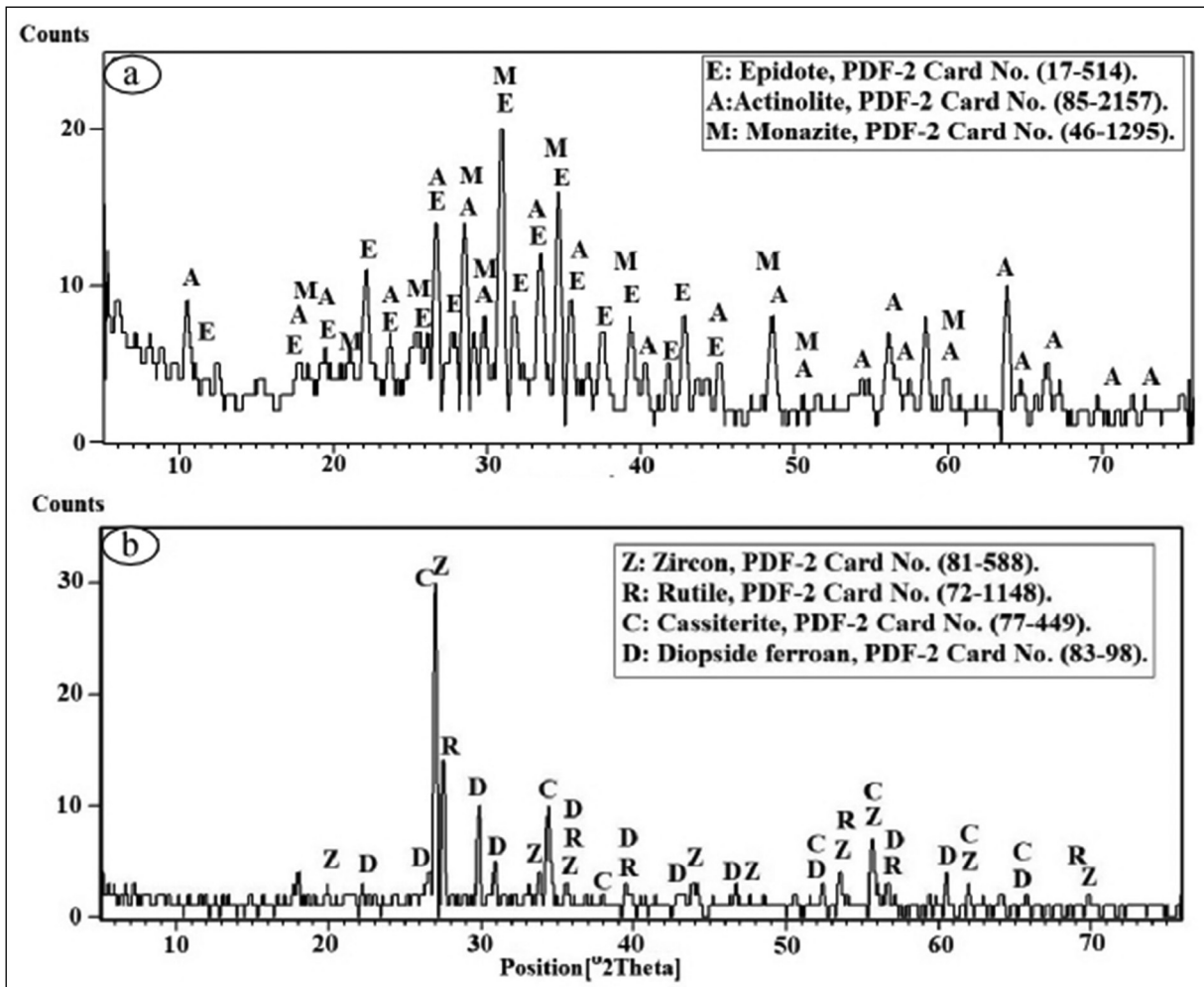
Figure 13- XRD diffractograms showing: a) epidote, actinolite and monazite separated fraction at 2.5 amps as magnetic, and b) zircon, rutile, cassiterite, and diopside separated at 2.5 amps as non-magnetic fraction of the Wadi Shaàb representative sample.

tabling products (concentrate and tail) were used in the bromoform-separation test to estimate the heavy mineral material balance and the data were presented at Table 4.

It is clear from the results shown in Table 3 that the heavy mineral assay increased from 7.63% of the feed sample to 45.03% in the concentrate after multi-stages gravity separation, while the heavy mineral recovery in the roughing stage reached to 62.64% and increased

Table 3- Material balance of the different products of gravity concentration via shaking table for Shaàb head sample.

Products of Tabling		Yield (%)	Heavy Mineral Assay (%)	Heavy Mineral Recovery (%)
Concentrate	Roughing stage	8.99	53.17	62.64
	Scavenging Round 1	3.45	47.79	21.63
	Scavenging Round 2	1.3	31.17	5.31
	Total Concentrate	13.74	45.03	89.58
Tail	Total	86.26	1.53	10.42
Feed	Total	100	7.63	100

Table 4- Feed and concentrate grade EDXRF analyses as well as enrichment ratio (E.R.) for the Shaàb test sample as results of gravity concentration via shaking table.

	Feed Grade	Concentrate Grade	Enrichment Ratio (E.R.)
Major Oxides in %			
Fe_2O_3	2.85	7.78	2.73
CaO	2.32	4.6	1.98
TiO_2	0.41	1.34	3.27
P_2O_5	0.087	0.125	1.44
K_2O	0.81	0.66	0.81
MnO	0.0537	0.15	2.79
Trace Elements in ppm			
Cr	377	1550	4.11
Zr	355	849	2.39
Ni	150	221	1.47
Co	110	279	2.54
V	142	253	1.78
Zn	65	119	1.83
Y	21	55	2.62
Pb	11	14	1.27
Cu	28	33	1.18
Th	<0.1	12.6	126
U	<0.1	11.2	112

to 89.58% after two stages of scavenging in a yield of 13.74% out of the feed sample.

EDXRF spectrometric analysis of final concentrate versus head sample analysis and enrichment ratio values are presented in Table 4 where the enrichment ratio values which were estimated by dividing the concentrate grade by the feed grade (c/f) and the resulting value indicates how many times the concentrate has element concentration relative to the feed. The enrichment ratio values for major elements such as Fe_2O_3 and TiO_2 showed a clear improvement and increased by 2.73% for Fe_2O_3 and 3.27 for TiO_2. As for the trace elements such as Zr, Cr, Co, Y, U, and Th, they showed high enrichment ratio values, as a result of doubling of the content of minerals bearing them as magnetite, ilmenite, rutile, sphene,

zircon, xenotime, almandine, and monazite in the concentrate.

4.2.2. Magnetic Separation

The heavy mineral fractions were used as feed for LIMS for separation of magnetite as a ferromagnetic mineral fraction and the non-magnetic fraction were subjected to HIMS to fractionate free-magnetite mineral fraction into paramagnetic and diamagnetic fractions. Four magnetic fractions were resulted; magnetite fraction, paramagnetic fraction separated at 0.8A, paramagnetic fraction separated at 1.5A, and paramagnetic fraction at 2.5A. Non-magnetic fraction separated at 2.5A was also obtained.

Magnetite Separation: Using a low intensity magnetic separator, magnetite is the separation product of this fraction and it represents about 0.30% mass of the heavy mineral fraction. The magnetite fraction was confirmed by SEM analyses where the Back-scattered electron (BSE) image with corresponding energy dispersive spectrum (EDS) and its stereo microscopic image were shown at Figures 14a, b respectively. The SEM data for magnetite as separate grain was depicted in Figure 14c.

Magnetic Fraction at 0.8A: Ilmenite is the main target mineral for separation in this fraction using HIMS at 0.8A that represents about 2.58% mass of the heavy mineral fraction. The BSE image and its corresponding EDS for this fraction as well as the stereo microscopic images are shown at Figure 15a, b respectively, they were clarified that the main content is iron (38.0%), titanium (27.4%), and silicon (18.8%), this means that ilmenite is the main constituents with traces of almandine garnet. Ilmenite as a separate grain was presented in Figure 15c.

Magnetic Fraction at 1.5 A: Garnet and leucoxene are the main essential minerals for separation in this fraction that represents about 2.18% mass of the heavy fraction of the Shaàb sample. The SEM data shown in Figure 16a as well as the stereo microscopic image shown in Figure 16b proved that leucoxene and almandine with traces of heavy silicates are the main minerals that have been occurred. SEM data concerning almandine is shown in Figure 16c.
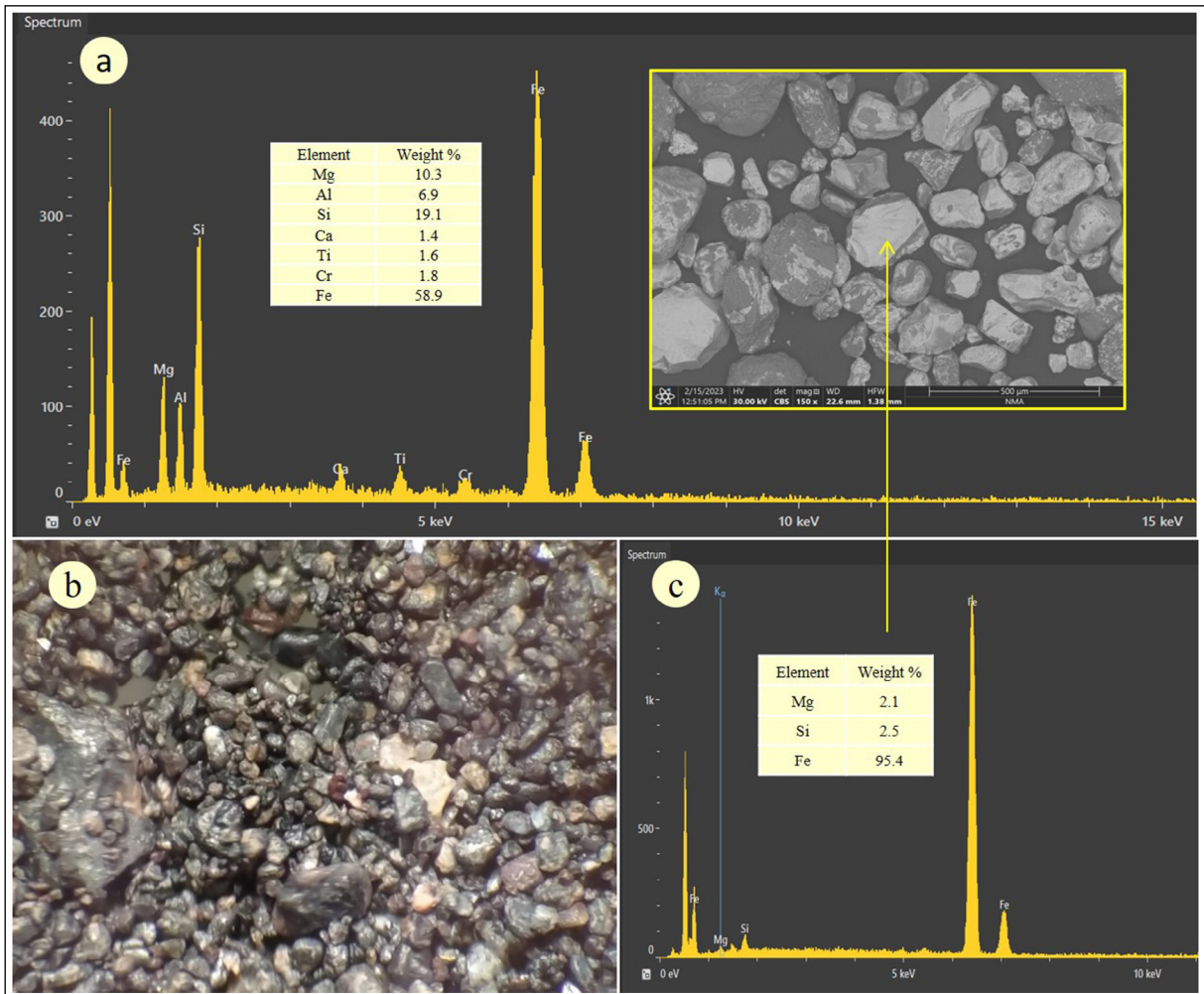
Figure 14- Representative back-scattered electron (BSE) image with corresponding EDS spectra, and stereo microscopic image for magnetite fraction a), b) respectively and c) for magnetite.

Magnetic Fraction at 2.5 A: Heavy silicates as pyroxene, amphibole and epidote are the target mineral for separation in this fraction as well as traces of monazite and xenotime. This heavy fraction represents about 1.49% mass of the heavy concentrate. The SEM results (Figure 17a) and stereo microscopic image (Figure 17b) proved that this fraction contains mainly heavy silicate minerals, in addition to the presence of monazite confirmed in Figure 17c.

Non-magnetic Fraction at 2.5 A: Non-magnetic minerals such as zircon, rutile, sphene, and cassiterite are the main heavy minerals can be separated at this fraction. This fraction represents about 7.19% mass of the heavy mineral fraction. The SEM data in Figure 18a proved that the main elemental content is Ti (32.0%), Si (29.4%), Ca (22.8%), and P (1.8%). The stereo microscopic image in Figure 18b as well as SEM data in Figures 18c, d, and e confirmed that zircon, rutile, and cassiterite are the essential minerals in this fraction.

A schematic sequence for processing and separating economic heavy minerals from the Shaàb stream sediments sample with material balance is presented as a flow-sheet in Figure 19.
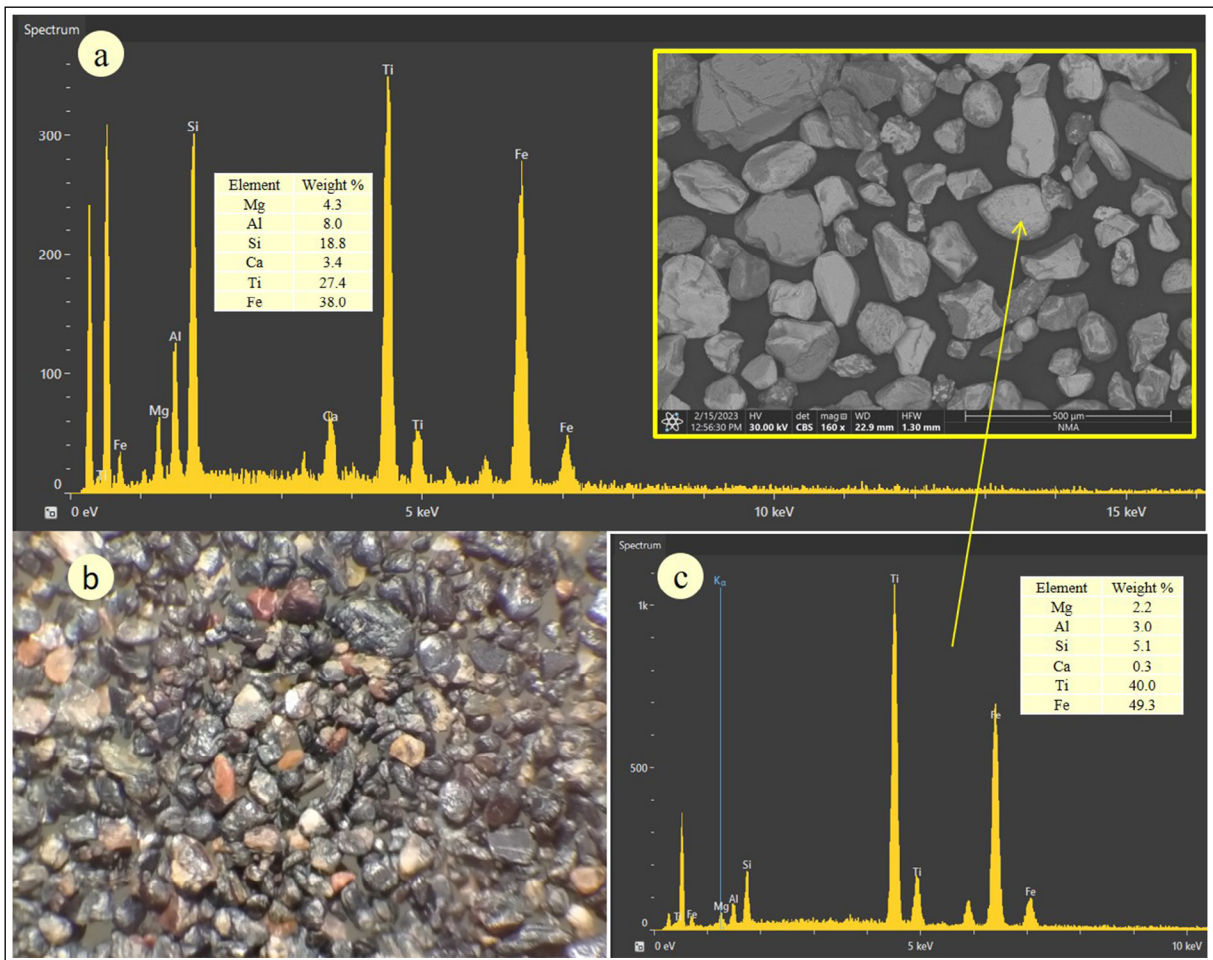
Figure 15- Representative BSE image with corresponding EDS spectra, and stereo microscopic image for magnetic fraction at 0.8A a), and b) respectively and c) for ilmenite.
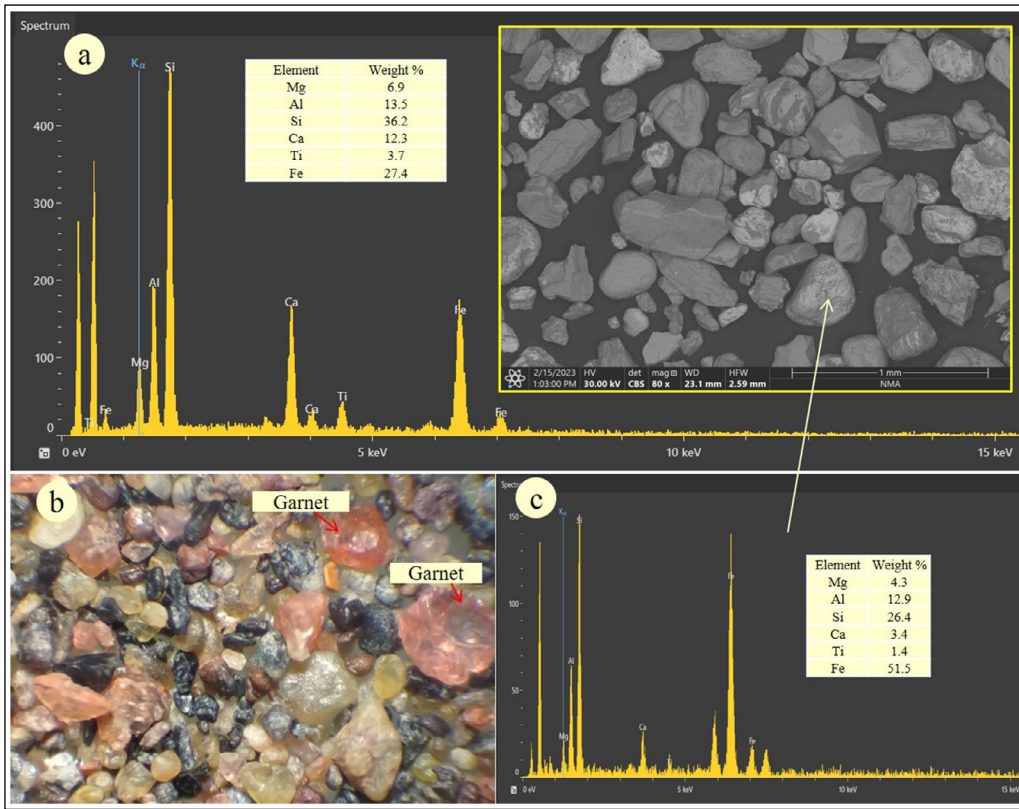
Figure 16- Representative BSE image with corresponding EDS spectra, and stereo-microscopic image for magnetic fraction at 1.5A a), b) respectively, and c) for almandine.
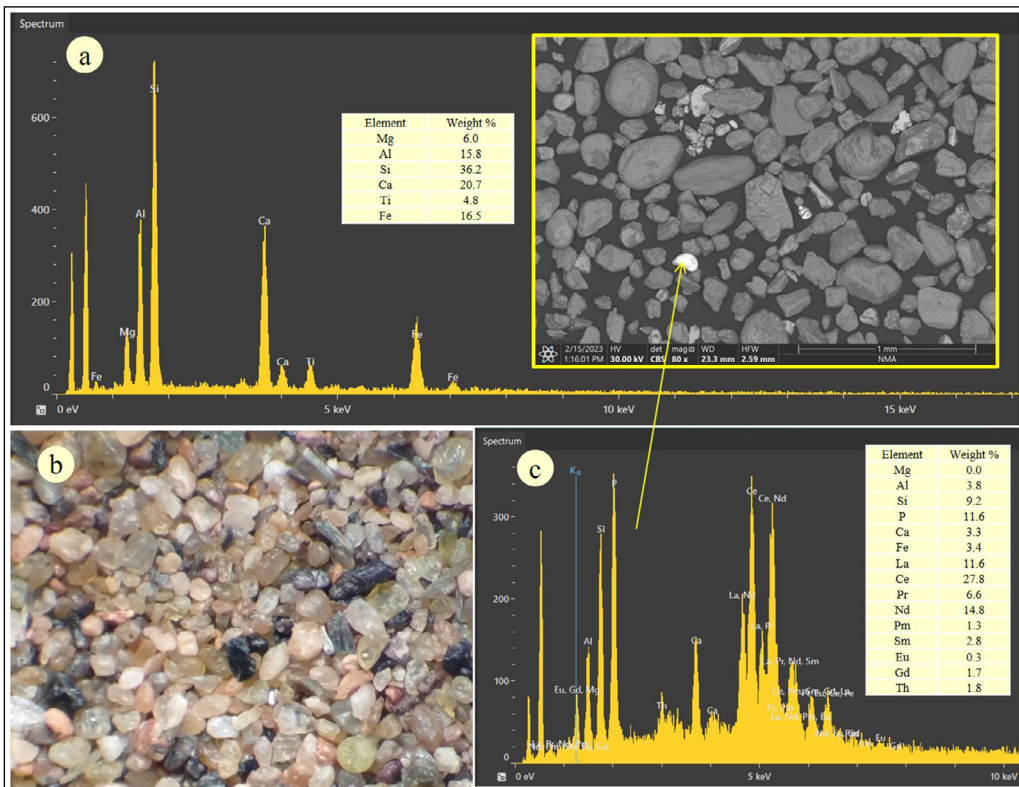

Figure 17- Representative BSE image with corresponding EDS spectra, and stereo microscopic image for magnetic fraction at 2.5A a), and b) respectively, and c) for monazite.
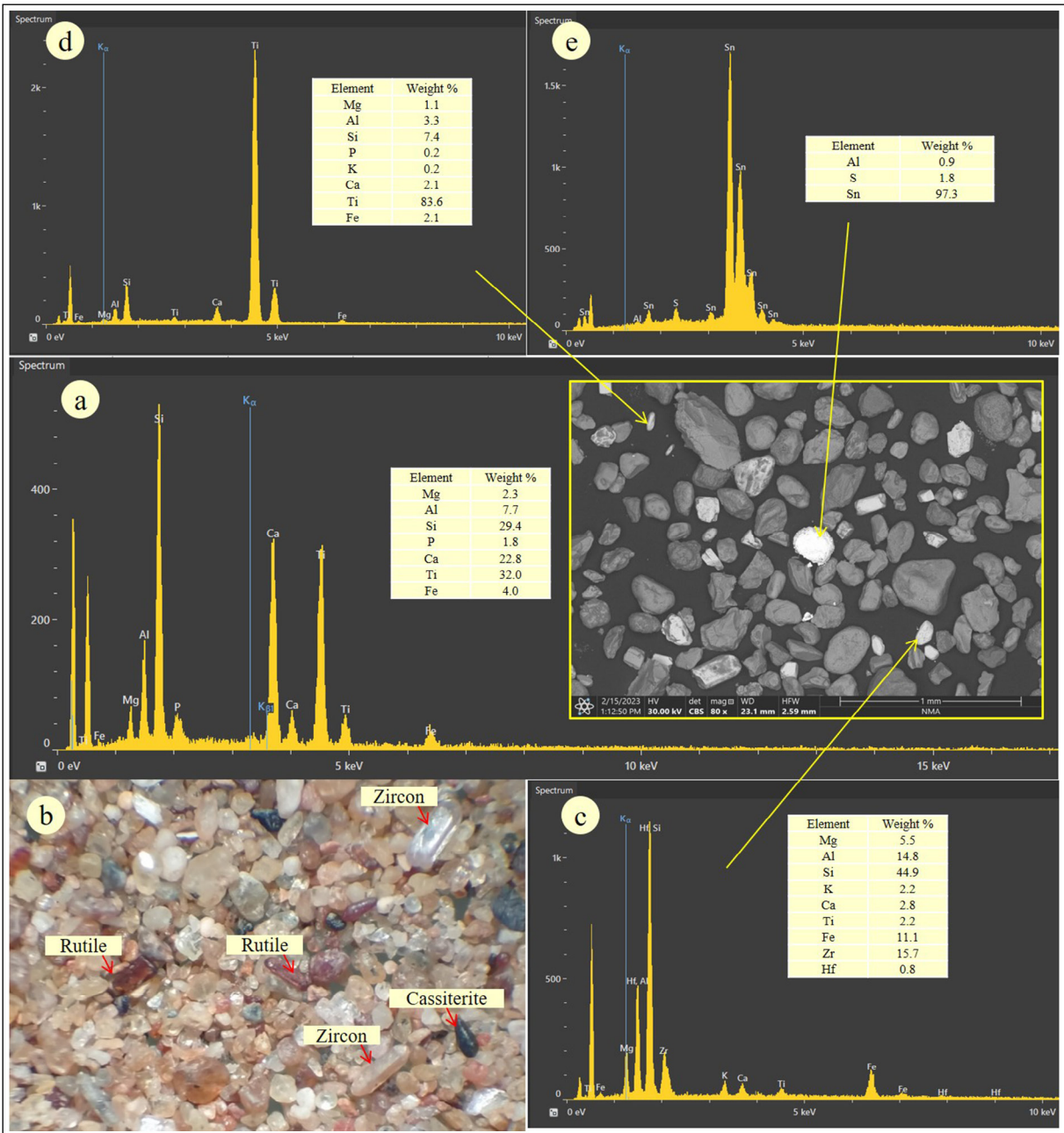
Figure 18- Representative BSE image with corresponding EDS spectra, and stereo icroscopic image for non- magnetic fraction at 2.5A a), and b) respectively, c) for zircon, d) for rutile, and e) for cassiterite.
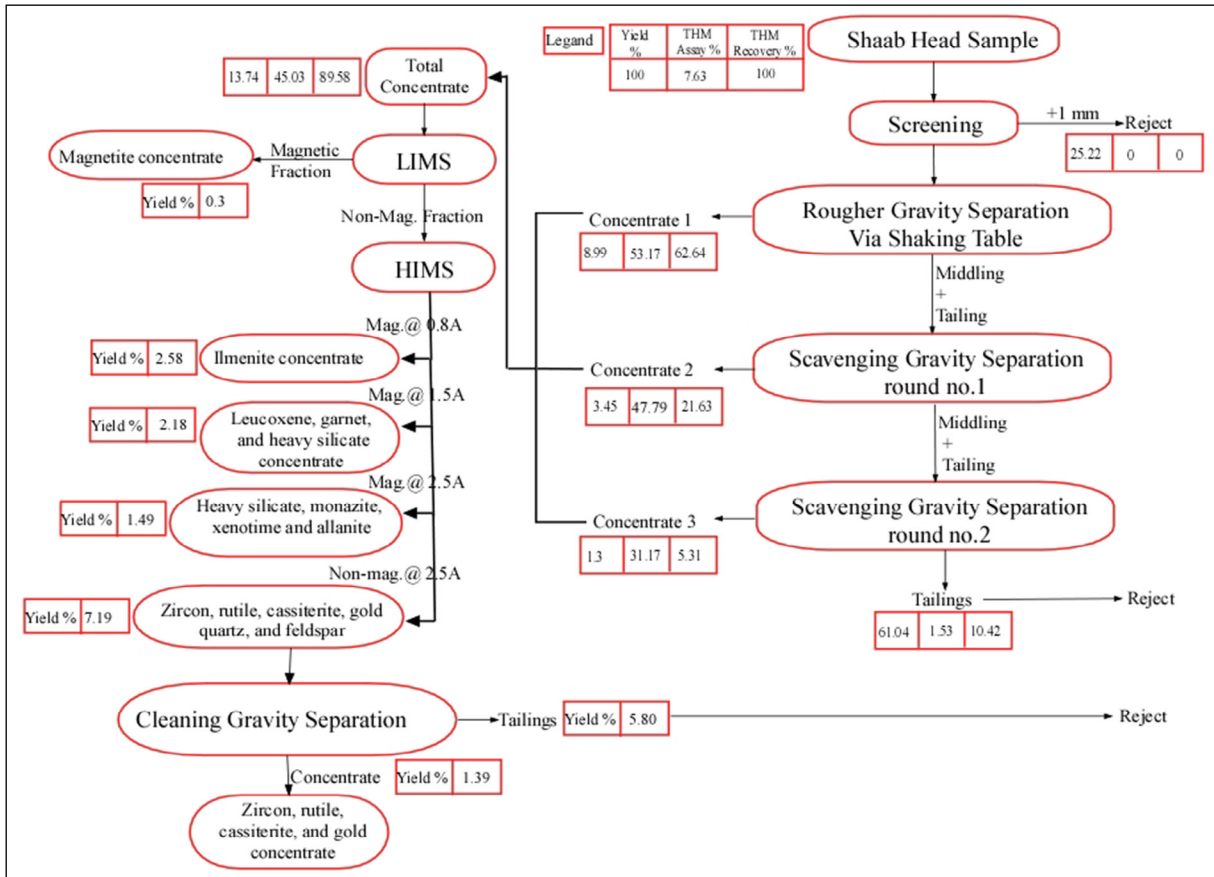
Figure 19- Flow-sheet with material balance for recovery of economic heavy minerals from Shaàb test sample.

5. Results

Mineralogical investigation of the Wadi Shaàb stream sediments revealed the presence of total heavy minerals content ranged from 2.91% mass to 11.24% mass with an average of about 8.00% mass. Microscopic examination supplemented with (XRD) and (SEM) analyses confirmed the presence of ilmenite, leucoxene, rutile, sphene, zircon, Zn-Sn-Pb minerals, xenotime, monazite and cassiterite. The estimated reserve of the economic heavy minerals within the Wadi Shaàb stream sediments can be summed up as follows; magnetite 3850 tons, zircon 669 tons, rutile 585 tons, leucoxene 585 tons, ilmenite 502 tons, almandine 184 tons, cassiterite 66 tons, xenotime 33 tons and monazite 3 tons. Physical upgrading processes of VHMs from the Wadi Shaàb stream sediments was successfully performed in this study using wet gravity concentration in conjunction with magnetic separation. The total heavy mineral assay increased from 7.63% to 45.03% after two rounds of the scavenging concentration step following the roughing step in a yield of 13.74% out of the original sample. Magnetite is the separation product of this fraction using a low intensity magnetic separator. DHIMS succeeded in fractionate free-magnetite mineral fraction into paramagnetic and diamagnetic fractions.

References

Diab, M., Abu El Ghar, M. A., Gaafar, I. M., El shafey, A. M., Hussein, A.W., Fawzy, M. M. 2022. Potentiality of Physical Upgrading for Valuable Heavy Minerals from Sermatai Area, Egypt. Journal of Mining and Environment 13, 1, 15-32.

EGSMA 2002. Egyptian geological survey and mining; geologic map of the Marsa Shaab, quadrangle, Egypt, scale 1:250 0000. Geological Survey, Cairo, Egypt.

Fawzy, M. M. 2018. Surface characterization and froth flotation of fergusonite from Abu Dob pegmatite using a combination of anionic and nonionic collectors. Physicochemical Problems of Mineral Processing 54(3), 677-687.

Fawzy, M. M. 2021*a*. Separation of fine beryl from quartz via magnetic carriers by the aiding of non-ionic surfactant. Physicochemical Problems of Mineral Processing 57(2), 14-23.

Fawzy, M. M. 2021*b*. Flotation separation of dravite from phlogopite using a combination of anionic/ nonionic surfactants. Physicochemical Problems of Mineral Processing 57(4), 87-95.

Fawzy, M. M., Abu El Ghar, M. S., Gaafar, I. M., El Shafey, A. M., Diab, M., Hussein, A. W. 2022*a*. Diit Quaternary Stream Sediments, Southern Coast of the Red Sea, Egypt: Potential Source of Ilmenite, Magnetite, Zircon, and Other Economic Heavy Minerals. Mining, Metallurgy and Exploration 39:655–667.

Fawzy, M. M., Abu El Ghar, M. S., Gaafar, I. M., El shafey, A. M., Diab, M., Hussein, A. W. 2022*b*. Recovery of valuable heavy minerals via gravity and magnetic separation operations from Diit Quaternary stream sediments, southern coast of the Red Sea, Egypt. International Conference on Chemical and Environmental Engineering, Journal of Physics: Conference Series; 2305 012020.

Grosz, A. E., Schruben, P. G. 1994. NURE geochemical and geophysical surveys; defining prospective terranes for United States placer exploration (No. 2097). USGPO; for sale by US Geological Survey, Information Services, Retrieved February 26, 2014.

Hegde, VS., Shalini, G., Kanchanagouri D. G. 2006. Provenance of heavy minerals with special reference to ilmenite of the Honnavar beach, central west coast of India. Current Science (00113891) 91 (5).

Jordens, A., Cheng, Y. P., Waters, K. E. 2013. A review of the beneficiation of rare earth element bearing minerals. Mineral Engineering 2013, 41, 97–114.

Iranmanesh, M., Hulliger, J. 2017. Magnetic separation: Its application in mining, waste purification, medicine. biochemistry and chemistry. Chemical Society Reviews 2017, 46, 5925–5934.

Moscoso-Pinto, F., Kim, H. S. 2021. Concentration and Recovery of Valuable Heavy Minerals from Dredged Fine Aggregate Waste. Minerals 11, 49.

Paltekar, M., Hegde, VS., Hulaji, S., Pratihari, AR., Korkoppa, MM. 2021. Geochemistry of heavy minerals from Uttara Kannada beach sediments, West Coast of India: An insight into provenance studies. Journal of Sedimentary Environments 6, 693-705.

Rahman, M. A., Zaman, M. N., Biswas, P. K., Sultana, S., Nandy, P. K. 2015. Physical separation for upgradation of valuable minerals: A study on sands of the Someswari river. Bangladesh J. Sci. Ind. Res. 50(1), 53-58, 2015

Rejith, R. G., Sundararajan, M. 2018. Combined magnetic, electrostatic, and gravity separation techniques for recovering strategic heavy minerals from beach sands. Marine Georesources & Geotechnology 35, 959–965.

Rydberg, J. 2014. Wavelength dispersive X-ray fluorescence spectroscopy as a fast, non-destructive and cost-effective analytical method for determining the geochemical composition of small loose-powder sediment samples, Journal of Paleolimnology 52:265–276.

Shalini, G., Hegde, V. S., Soumya, M., Korkoppa, M. M. 2020. Provenance and Implications of Heavy Minerals in the Beach Sands of India's Central West Coast, Journal of Coastal Research 36 (2), 353-361.

Yousef, A. F., Salem, A. A., Baraka, A. M., Aglan, O. Sh. 2009. The impact of geological setting on the groundwater occurrences in some wadis in Shalatein-Abu Ramad area, south Eastern Desert, Egypt. European Water 25 (26), 53-68.

Yu, C., Cheng, Jing-J., Jones, L., Wang, Y., Faillace, E., Loureiro, C., Chia, Y. 2023. Data collection handbook to support modeling the impacts of radioactive material in soil. 10.2172/10162250.

Zhao, W. Z., Lu, B., Yu, J. B, Zhang, B. B., Zhang, Y. 2020. Determination of sulfur in soils and stream sediments by wavelength dispersive X-ray fluorescence spectrometry. Microchemical Journal 156:104840.